

# The effect of aluminium oxide on the residual voltage of ZnO varistors

Mourad Houabes<sup>\*</sup>, Slavko Bernik<sup>1</sup>, Chabane Talhi, Ai Bui

*Laboratoire de Génie Electrique, Université Paul Sabatier de Toulouse, 118 route de Narbonne, 31062 Toulouse, France*

Received 2 April 2004; received in revised form 24 May 2004; accepted 10 September 2004

Available online 9 December 2004

## Abstract

The role of aluminium oxide is investigated in an attempt to obtain low residual voltage ZnO varistors fabricated in the traditional way. The samples were sintered at three different temperatures: 1150, 1200, and 1250 °C for three different times: 1, 2, and 3 h. The effect of aluminium additions, in the range of 500–10,000 ppm, on the characteristics of electric field–current density was investigated. Addition of Al<sub>2</sub>O<sub>3</sub> shifts the upturn region to higher current density due to the increase of the conductivity of the ZnO grains up to an optimal value. After 1000 ppm, the beneficial effect on the onset of upturn voltage is no more efficient. This work highlighted the ambivalent role of aluminium (donor or acceptor) and the need for tuning both an optimal concentration and sintering time to obtain the greatest conductivity. Our results suggest that Al<sup>3+</sup> substitutes first to Zn<sup>2+</sup> sites in the ZnO wurtzite structure and then, when thermodynamic saturation is reached, interstitial sites.

© 2004 Elsevier Ltd and Techna Group S.r.l. All rights reserved.

**Keywords:** C. Electrical properties; E. Varistors; ZnO-based ceramics

## 1. Introduction

ZnO-based ceramics containing such additives as Bi<sub>2</sub>O<sub>3</sub>, Sb<sub>2</sub>O<sub>3</sub>, CoO, MnO, and Cr<sub>2</sub>O<sub>3</sub> are known to exhibit high non-ohmic behaviour in their current–voltage (*I*–*V*) characteristics [1]. This non-linear property (Fig. 1) allows their use for the protection against transient surge of overvoltage [1,2]. The varistors are produced by a ceramic sintering process that gives rise to a structure comprised of conductive ZnO grains (≈10 μm) surrounded by extremely thin layer (≈100 nm) between the ZnO grains [3]. Varistor action is controlled by depletion layers situated within the ZnO grains at grain–grain interfaces [2].

The *I*–*V* characteristics of ZnO ceramics are expressed by the following empirical equation:

$$I = \left( \frac{V}{C} \right)^{\alpha} \quad (1)$$

where *V* is the voltage across the body and *I* is the current flowing through it. The non-linear resistance, *C*, is the constant corresponding to the resistance of ohmic resistor.  $\alpha$  is the voltage non-linear exponent [1].

The low-current region (I), denoted pre-breakdown, is ohmic [2]. The resistance of the ZnO grains is very small ( $\rho_g \approx 0.1$ – $10 \Omega \text{ cm}$ ). The current is mainly limited by the very high impedance of grain boundaries ( $\rho_j \approx 10^{10}$ – $10^{12} \Omega \text{ cm}$ ) [4].

The existence of the non-linearity region (II) is the most significant property of the varistors. The varistor presents its conducting phase here. The current increases much more quickly than the voltage. At high current densities, beyond  $10^3 \text{ A/cm}^2$ , the curve exhibits an upturn (III), *I*–*V* becomes again linear. The upturn represents the voltage drop in the grains [2], and restricts ZnO varistors application as lightning protection devices. Referring to the *I*–*V* characteristic, the properties that are ZnO grain specific will show up in the upturn region and those that are grain boundary specific will appear in the pre-breakdown region [5]. If donor doping reduces the grain resistance, the voltage increase will be retarded and the upturn will be delayed to

<sup>\*</sup> Corresponding author.

<sup>1</sup> Institut Jozef Stefan, Ljubljana, Slovenia.

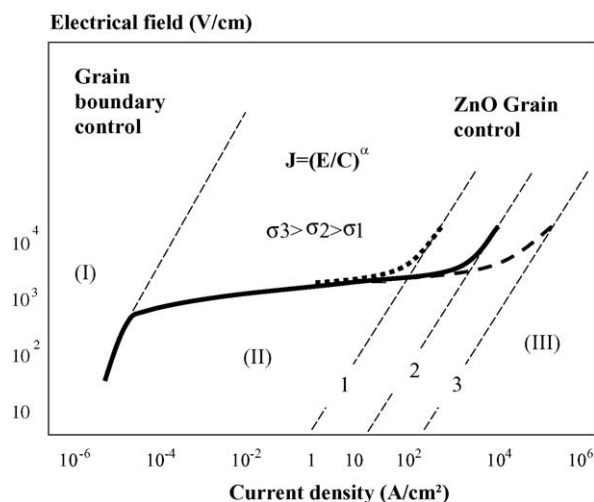


Fig. 1. ZnO varistors  $I$ – $V$  characteristic, with “iso-resistivity” lines superposition.  $\sigma$ : ZnO grains conductivity.

higher current densities [6]. It is known that donor ions such as  $\text{Al}^{3+}$ ,  $\text{Ga}^{3+}$  or  $\text{In}^{3+}$  can indeed delay the onset of upturn voltage [7,8].

To achieve a given breakdown voltage, the varistors thickness and the grain size can be changed [9,10]. The lightning protector application calls for ZnO varistors blocks with a thickness of several cm which is obtained by piling up in series a number of blocks. Thus, the residual voltage of the device depends on the current which crosses the varistors piled up, i.e., ZnO ceramic and contacts, and also on their total height. Therefore, decreasing the thickness of each varistor contributes not only to the reduction of the height of the lightning protector but also to the reduction of the residual voltage. The aim of this work is to reduce the varistor residual voltage by elaboration of ceramics presenting ZnO grains with both higher conductivity and lower size.

The breakdown voltage depends in part on the grain size, i.e., the chemical composition and the heat treatment used for sintering [11,12]. However, the role and the position of aluminium is not yet completely elucidated [13,14]. In this paper, we report a detailed study on the aluminium doping and the observed electrical properties.

## 2. Experimental details

### 2.1. Samples preparation

The samples were produced by conventional ceramic technology, which begins with weighing, mixing, and milling of oxide powders in ball mills. After addition of organic binder substances, the aqueous slurry is spray-dried to produce granulate which are sieved to extract dust and large agglomerated particles. The material is then pressed into pellets under pressure of  $350 \text{ kg/cm}^2$  and sintered at different temperatures: 1150, 1200, and  $1250^\circ\text{C}$ . Three

sintering times were used: 1, 2, and 3 h. The ZnO varistors disks, having 3.1 cm diameter and 5 mm thickness, were polished, electrotyped at  $750^\circ\text{C}$  for 1 h and coated by a polymeric material. The reference composition was:  $(93.336 - x) \text{ mol\% ZnO} + 0.803 \text{ mol\% (Bi}_2\text{O}_3 + \text{MnO} + \text{Cr}_2\text{O}_3 + \text{NiO}) + 2.810 \text{ mol\% Sb}_2\text{O}_3 + 0.442 \text{ mol\% CoO} + 0.1 \text{ mol\% (MgO} + \text{B}_2\text{O}_3) + x \text{ mol\% Al}_2\text{O}_3$  (where  $x$  varies from 500–10,000 ppm).

### 2.2. $I$ – $V$ measurements

For values of current lower than 1 mA, the current–voltage  $I$ – $V$  characteristics were measured by using a system consisted of a regulated voltage generator (FUG HCN 350–12500), micro processing digital multimeter (Racal Dana 6000) and an ammeter (Keithley 619). For more than 1 mA, the pulse current generator and an oscilloscope (Tektronix 2430) were used in order to avoid the thermal runaway.

### 2.3. Analysis of microstructure

For the microstructure examination, cross-sections of the samples were ground and polished. Half of the polished surface of each sample was etched in diluted hydrochloric acid to expose the ZnO grains for analysis of their average size. Microstructures were analysed using a scanning electron microscope (SEM). Phases observed in the samples were identified by energy-dispersive X-ray spectroscopy (EDS). The average ZnO grains size was determined from measurements of 200–300 grains per sample. The program used is based on the method of interceptions [15].

## 3. Results and discussion

Two microstructures of samples sintered at  $1200^\circ\text{C}$  for 1 h and X-ray analysis are given in Figs. 2–4. The samples have similar microstructure composed of  $\text{ZnO}(\text{Co}, \text{Mn})$  grains,  $\text{Bi}_2\text{O}_3(\text{Zn}, \text{Cr}, \text{Co}, \text{Mn}, \text{Ni})$ -rich phase and  $\text{Zn}_7\text{Sb}_2\text{O}_{12}$  (Al, Cr, Mn, Ni, Co) spinel-type phase. The ZnO grain size depends on the sintering temperature and the sintering time. For a given composition average grains size is obviously larger in samples sintered at higher temperature for longer periods. Al is detected in a prevalent way in the spinel phase. Its amount in the spinel phase correlates to the amount of Al added to the starting composition (Fig. 4). However, the ZnO grains sizes are similar in all samples sintered at  $1200^\circ\text{C}$  for 1 h regardless the amount of Al added (Table 1).

The grains sizes depends only on amount of spinel phase located at the grain boundaries and therefore on the antimony doping level [16].

Fig. 4 shows the varistor effect obtained for all the  $I$ – $V$  characteristics, whatever the content, for the same sintering conditions (temperature =  $1200^\circ\text{C}$  and time = 1 h). Practically, the same  $I$ – $V$  characteristic form is obtained for all the others sintering conditions. For example, the saturation

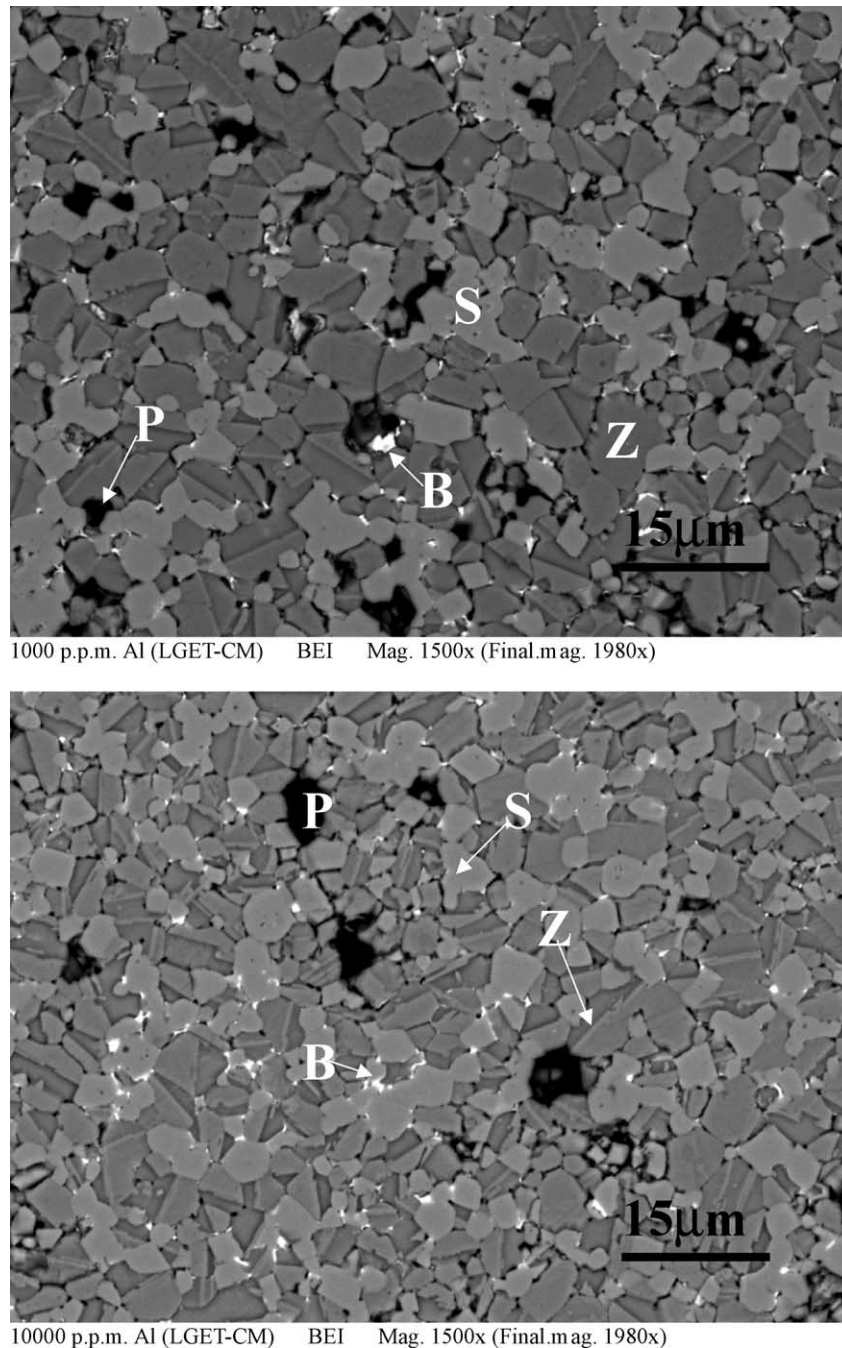


Fig. 2. Backscattered electron (BE) images of samples doped with 1000 ppm (top) and 10,000 ppm (bottom) of Al. Z: ZnO phase; S:  $\text{Zn}_7\text{Sb}_2\text{O}_{12}$  spinal phase, B:  $\text{Bi}_2\text{O}_3$ -rich phase, P: pore.

region always moves away to higher currents. We observe an optimal value of the Al content in the range 500–1000 ppm: the conductivity is the highest. For the same concentration of Al, an optimum value is also found relative to the sintering

time (Fig. 5). Upturn goes up for two hours and down again for three hours. However, compared to the sintering temperature variation ambivalence does not appear. Conductivity always increases when the temperature increases (Fig. 6).

ZnO is well known for its non-stoichiometry due to the zinc atoms interstitial sites. It is commonly accepted that the ZnO exhibits an oxygen vacancies. With these intrinsic defects, ZnO is a high n-doped semiconductor [17,18]. These defects introduce donor states in the forbidden band slightly below the conducting band, reduce the gap (3.2 eV)

Table 1  
Average ZnO grains size ( $D$ ) and its standard deviation ( $\nu$ ) for the samples with 1000 and 10,000 ppm of Al

Sample Al (ppm)	Number of grains	$D$ ( $\mu\text{m}$ )	$\nu$ ( $\mu\text{m}$ )	$\nu$ (%)
1,000	374	3.5	1.3	37
10,000	382	3.2	1.1	34

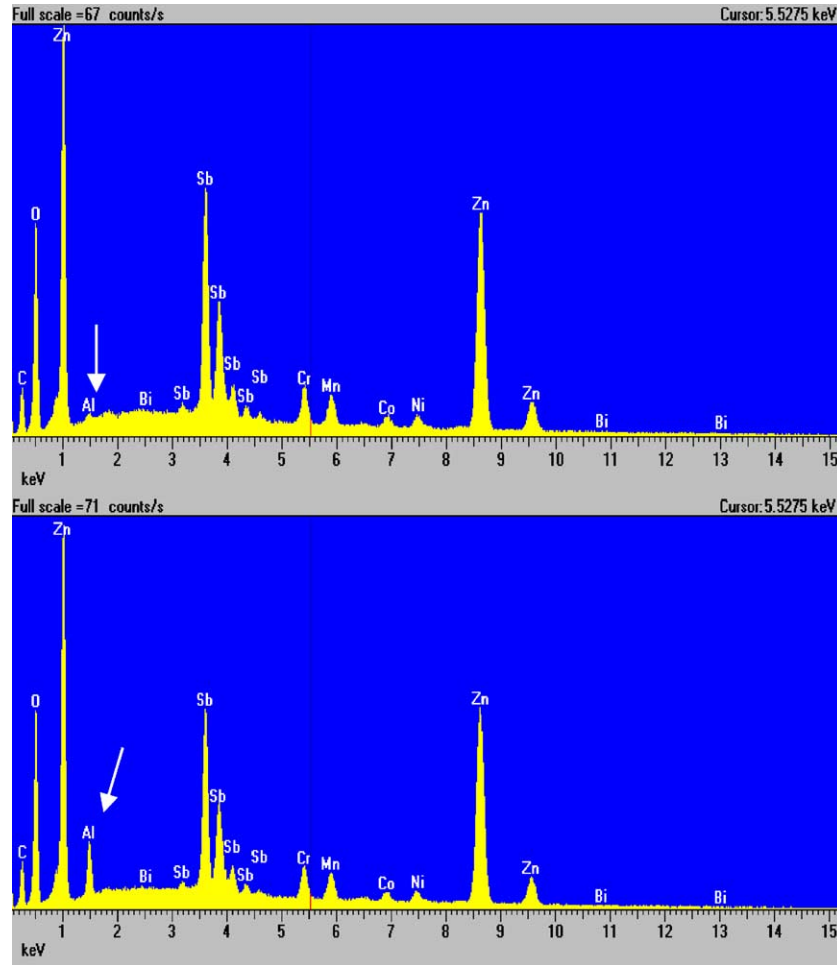


Fig. 3. Spinel phase EDS Spectra in the samples doped by 1000 ppm (top) and 10,000 ppm (bottom) of Al.

and result in the conducting behaviour of ZnO. The donors are assumed to be interstitial zinc ions  $Zn_i$ . The donor density is about  $10^{17}$ – $10^{19}$   $cm^{-3}$  and the resistivity 0.1–10  $\Omega$  cm [4].

Neutral  $Zn_i^x$  interstitial zinc atom ionises first as [6]:

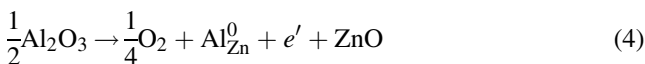


and then second once such as:



where  $Zn_i^0$  and  $Zn_i^{00}$ , are respectively once and twice ionised interstitial zinc atoms.

Such free electron  $e'$  moves to the conducting band and enhance the ZnO conductivity which can be further increased by the extrinsic defects. When ZnO is doped with aluminium, Al atoms enter the ZnO structure and replace Zn atoms at regular sites such as [6]:



$Al_{Zn}^0$  is aluminium atom in zinc atom substitution site, ionised once. In Zn substitutions with Al free electrons are

released and raise the conductivity  $\sigma$  by increasing the electron density as:

$$\sigma = ne\mu \quad (5)$$

where  $n$  is the number of electrons coming from the reactions 2 and 3,  $e$  is the electron charge, and  $\mu$  is its mobility. The negative charge carriers are considered to be the majority carriers.

The electron liberated by the Al in reaction 4 adds to the number of free electrons  $n$  and increases the conductivity. In this case Al acts as donor. Furthermore, Al force Zn atoms by substitution from their regular sites to the interstitial site and additional free electrons are released according to reactions 2 and 3.

However, Al atom can also enter the structure and have preference for interstitial sites, both directly and indirectly by substituting Zn on its regular site at first and then moving to the interstitial position. At interstitial position the aluminium absorbs an electron such us [6]:





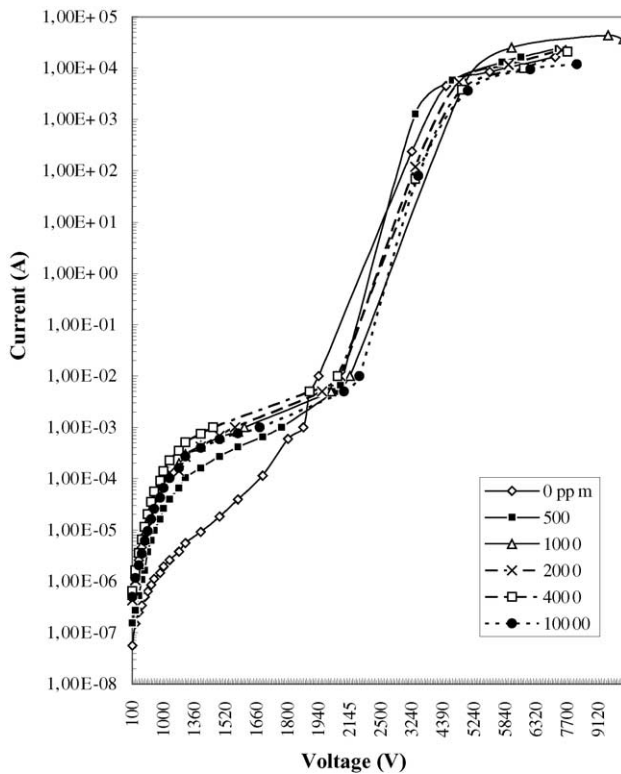


Fig. 4.  $I$ - $V$  characteristics of samples: without Al, 500, 1000, 2000, 4000, and 10,000 ppm Al added. Sintering temperature = 1150 °C and sintering time = 1 h.

$Al_i'$  is ionised once aluminium atom in interstitial site, and  $h^0$  hole positive charge.

In this case the aluminium behaves as an acceptor and decreases the conductivity. With an increasing amount of Al incorporated into the zinc oxide crystal lattice, the Al is accommodated both substitutionally and interstitially, and soon a thermodynamic condition may be reached (saturation of zinc sites) where Al preferentially occupies interstitial sites that the Zn would otherwise occupied. It is worth noting that the crystal structure of ZnO wurtzite structure has relatively large interstices which can readily accommodate excess zinc interstitially ( $Zn^{2+}$ :  $74 \times 10^{-12}$  m) or ( $Al^{3+}$ :  $51 \times 10^{-12}$  m). The acceptor effect of Al dominates its donor effect and the conductivity decreases. The donor and acceptor behaviour of Al was thoroughly elaborated and reported by Gupta [4].

In this work, the ambivalent role of aluminium, regarding the grain conductivity, is checking for different sintering times. Diffusion of aluminium into zone wurtzite structure needs time and can therefore influence which sites  $Al^{3+}$  will preferentially occupy. This affects the donor or acceptor behaviour of  $Al^{3+}$  and can explain the conductivity variation of samples in respect to level of Al doping and sintering time. For the increase in sintering temperature, the thermoelectronic phenomenon gives higher mobility to the charge carriers and is the dominant parameter. Therefore, the conductivity keeps increasing in this case.

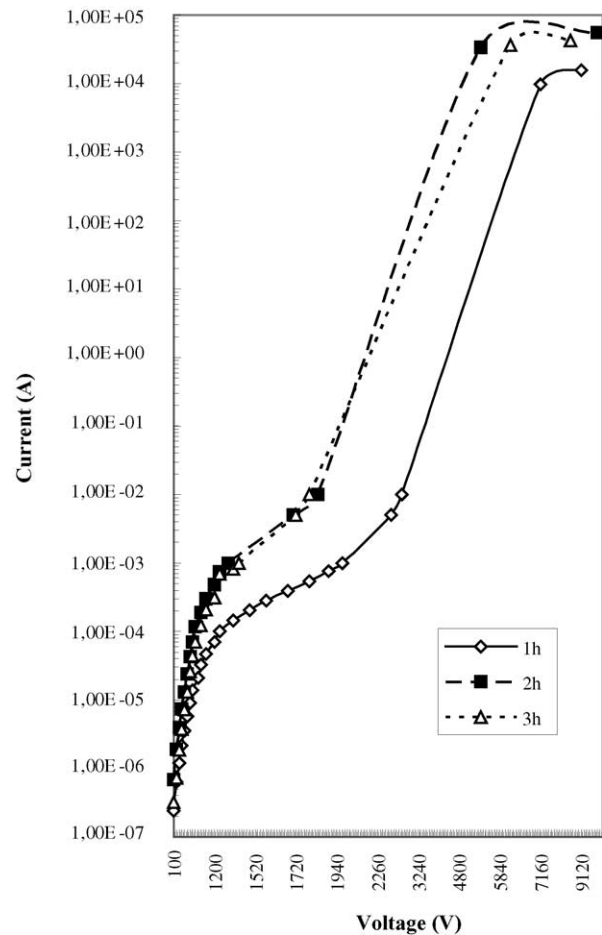


Fig. 5.  $I$ - $V$  characteristics for 2000 ppm Al added. Sintering temperature = 1200 °C and sintering time = 1, 2 and 3 h.

Measured values of threshold voltage  $V_s$  can be determined using  $I$ - $V$  characteristics. In fact  $V_s$  corresponds to a current equal to 1 mA (Tables 2 and 3).

The threshold voltage of the various samples is practically uninfluenced by variations in aluminium concentration. That is checked for all sintering times and temperatures. The values of the variance of threshold voltage are not too high and show that  $V_s$  is never very far from an average value connected to conditions of sintering given (temperature and time) (Table 4).

Table 2  
Threshold voltage  $V_s$  (V) measured for a leakage current of 1 mA for various sintering temperatures: 1150, 1200, and 1250 °C

$T$ (°C)	Al (ppm)					
	0	500	1000	2000	4000	$10^4$
1150	2170	2438	2100	1990	1930	2257
1200	1940	2070	2145	2100	2055	2227
1250	1580	1720	1705	1715	1580	1620

Sintering time = 1 h.

Table 3

Threshold voltage  $V_s$  (V) measured for a leakage current of 1 mA for various sintering times: 1, 2, and 3 h

$t$ (h)	Al (ppm)					
	0	500	1000	2000	4000	$10^4$
1	1940	2070	2145	2100	2055	2227
2	1665	1910	1880	1820	1880	1770
3	1595	1490	1790	1800	1810	1815

Sintering temperature = 1200 °C.

Table 4

Average threshold voltage measured and its variance for all sintering temperatures and times used

$T$ (°C)	$V_{sm}$ (V)	Variance, $v$ (V)	Variance (%)
1150	2147	185	8.6
1200	2089	96	4.5
1250	1653	67	4

$t$ (h)	$V_{sm}$ (V)	Variance, $v$ (V)	Variance (%)
1	2089	96	4.5
2	1821	91	5
3	1716	139	8.1

Knowing that the threshold voltage  $V_s$  and the ZnO grain size  $D$ , are proportionally connected by the relation [2,4]:

$$V_s = \frac{d}{D} V_{gb} \quad (7)$$

where  $d$  is the thickness of the varistor and  $V_{gb}$  the barrier voltage ( $\approx 2$ –4 V).

One concludes that the results from the microstructures analyses are confirmed by the threshold voltage experimental measurements. Aluminium does not have a great influence on the ZnO grains size, and thus practically no influence on the varistors threshold voltage.

The leakage current is the current value, which corresponds to a voltage equal to half of the threshold voltage  $V_s$ . This calculation will enable us to compare, the  $I$ – $V$  characteristic ohmic region evolution compared to the upturn region as a function of the aluminium concentration variation. The leakage current values for increasing aluminium concentration and sintering temperatures and times are presented in Tables 5 and 6.

Aluminium has an effect, not only on the upturn region controlled by ZnO grains resistance, but also, on the low-

Table 5

Leakage current ( $\mu$ A) for various sintering temperatures: 1150, 1200, and 1250 °C

$T$ (°C)	Al (ppm)					
	0	500	1000	2000	4000	$10^4$
1150	0.8	11	21	28	45	35
1200	1.8	30	95	113	150	110
1250	2.7	45	105	130	220	630

Sintering time = 1 h.

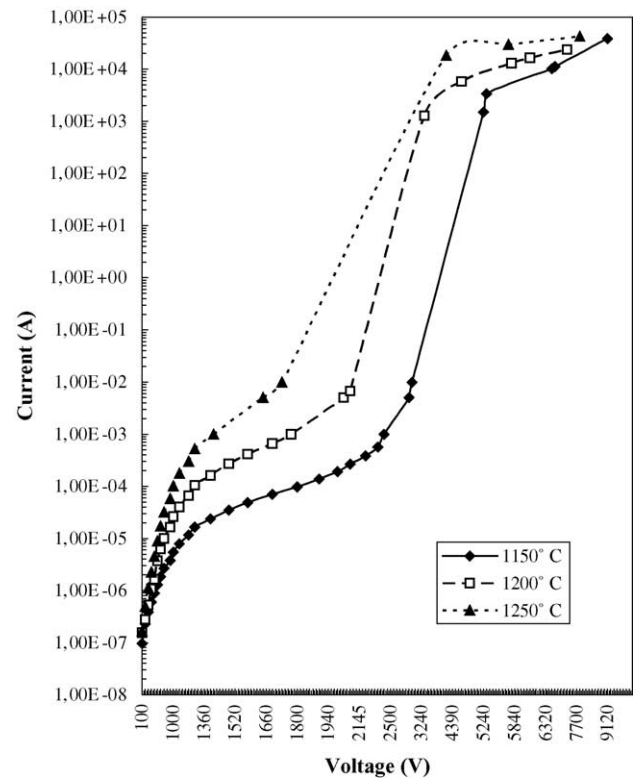


Fig. 6.  $I$ – $V$  characteristics for 500 ppm Al added. Sintering temperature = 1150, 1200, and 1250 °C and sintering time: 1 h.

current region that determines the leakage current value. The effect is relatively similar. When the Al concentration increases, the low-current region goes up and consequently the leakage current increases. Al plays a donor role. When the Al content keeps increasing, the low-current region goes down again and the leakage current decreases. In this case Al plays an acceptor role. However, this effect is accentuated more in the upturn region than in low-current region.

The upturn region is completely controlled by the ZnO grains resistance. The current is completely resistive. However, the low-current region is mainly controlled by the grain boundaries, and the current has resistive ( $I_R$ ) and capacitive ( $I_C$ ) components such as  $I_R \ll I_C$  [4]. So the aluminium influence on the ZnO grains conductivity appears also on the low-current region but with a less importance.

Fig. 7 shows the complete effect of Al. Its ambivalent effect on low-current region is also taken into account. This

Table 6

Leakage current ( $\mu$ A) for various sintering times: 1, 2, and 3 h

$t$ (h)	Al (ppm)					
	0	500	1000	2000	4000	$10^4$
1	1.84	30	120	130	150	110
2	0.85	33	110	120	185	220
3	1.4	22	105	71	3.5	1.9

Sintering temperature = 1200 °C.

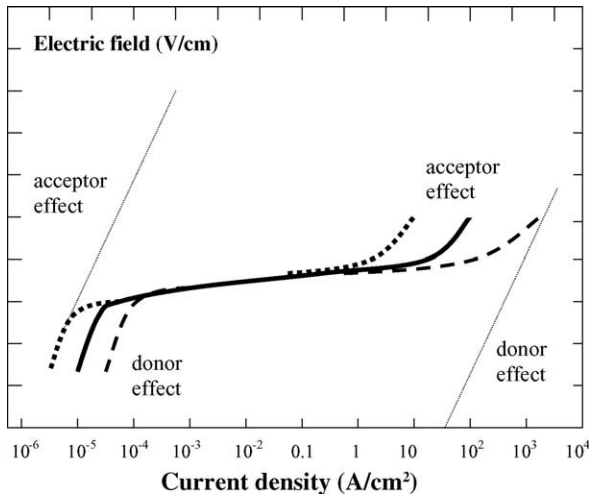


Fig. 7. Aluminium ambivalence effect (donor or acceptor) on the two regions: upturn and low-current, of ZnO varistors  $I$ – $V$  characteristics.

is explained by the fact that if the number of donor increases, the barrier of potential height  $\phi_B$  decreases, such as [15]:

$$\phi_B = \frac{e^2 N_S^2}{2\epsilon_0 \epsilon_r N_D} \quad (8)$$

where  $e$  is the electron charge;  $N_S$  is the density of surface states and  $N_D$  is the donor density;  $\epsilon_0$  is the dielectric constant in vacuum and  $\epsilon_r$  is the relative dielectric constant of ZnO.

A reduction of  $\phi_B$  does increase the density of current, such as [16,19]:

$$J = J_0 \exp \left( \frac{\sqrt{E e^3 / 4\pi \epsilon_0 \epsilon_r} - \phi_B}{K_B T} \right) \quad (9)$$

where  $J_0$  is a constant depending on material;  $E$  the applied electric field;  $K_B$  the constant of Boltzmann and  $T$  the absolute temperature.

When the sintering duration varies, aluminium also plays its ambivalence role. The leakage current increases up to a maximum value, then decreases. However, when the sintering temperature increases, the thermoelectronic effect supersedes the aluminium donor or acceptor role, and the leakage current keeps increasing.

#### 4. Conclusions

The influence of aluminium doping, sintering temperature and sintering time on ZnO grains conductivity and size was investigated.

- Aluminium penetrates in the spinel phase  $\text{Zn}_7\text{Sb}_2\text{O}_{12}$  with a quantity proportional to that added in the chemical

starting formulation. Nevertheless, the ZnO grains size is influenced only very little by the aluminium content.

- Aluminium has an ambivalent effect on ZnO grains conductivity. Whatever the parameter: sintering time or Al content a similar behaviour is observed: Al acts as donor then as acceptor. This could be explained by thermodynamic saturation of the zinc sites in ZnO wurtzite structure and then a preference for octahedral sites as interstitial location.

These results on conductivity are valid for the two regions of  $I$ – $V$  characteristic: the upturn region and with less importance the low-current region.

#### References

- [1] M. Matsuoka, Non-ohmic properties of zinc oxide ceramics, *Jpn. J. Appl. Phys.* 10 (6) (1971) 736–746.
- [2] L.M. Levinson, H.R. Philipp, Zinc oxide varistors—a review, *Am. Ceram. Soc. Bull.* 65 (4) (1986) 639–646.
- [3] D.R. Clarke, Grain boundary segregation in a commercial ZnO-based varistor, *J. Appl. Phys.* (50) (1979) 6829.
- [4] T.K. Gupta, Application of zinc oxide varistors, *J. Am. Ceram. Soc.* 73 (7) (1990) 1817–1840.
- [5] T. Miyashi, K. Maedo, K. Takahashi, T. Yamazaki, Effects of dopants on the characteristics of ZnO varistors, in: L.M. Levinson (Ed.), *Advances in Ceramics*, vol. 1, Grain Boundary Phenomena in Electronic Ceramics, Am. Ceram. Soc., Columbus, OH, 1981 pp. 309–315.
- [6] T.K. Gupta, Microstructure engineering through donor and acceptor doping in the grain and grain boundary of a polycrystalline semi-conducting ceramic, *J. Mater. Res.* 7 (12) (1992) 3280–3295.
- [7] W.G. Carlson, T.K. Gupta, Improved varistor nonlinearity via donor impurity doping, *Jpn. J. Appl. Phys.* 53 (8) (1982) 5746–5753.
- [8] T. Takemura, M. Kobayashi, Y. Takada, K. Sato, Effect of bismuth sesquioxide on the characteristics of ZnO varistors, *J. Am. Ceram. Soc.* 69 (5) (1986) 430–436.
- [9] J. Wong, Microstructure and phase transformation in a highly non-ohmic metal oxide varistor ceramic, *J. Appl. Phys.* 46 (4) (1978) 2407–2411.
- [10] T. Asokan, Effect of dopants' distribution on the non-linear properties of a ZnO-based non-linear resistor, *Br. Ceram. Trans. J.* (80) (1987) 187–189.
- [11] K. Eda, Conduction mechanism of non-ohmic zinc oxide ceramics, *J. Appl. Phys.* 89 (5) (1978) 2964–2972.
- [12] E. Olsson, L.K.L. Falk, G.L. Dunlop, R. Osterlund, The microstructure of the ZnO varistor, *J. Mater. Sci.* (20) (1985) 4091–4098.
- [13] K. Eda, Zinc oxide varistors, *I.E.E.E. Electric. Insulat. Mag.* 5 (6) (1989) 28–41.
- [14] M. Inada, Crystal phases of nonohmic zinc oxide ceramics, *Jpn. J. Appl. Phys.* 17 (3) (1978) 1–10.
- [15] W. Heywang, Resistivity anomaly in doped barium titanate, *J. Am. Ceram. Soc.* 47 (10) (1964) 484–490.
- [16] T. Takemura, M. Kobayashi, Y. Takada, K. Sato, Effects of antimony oxide on the characteristics of ZnO varistors, *J. Am. Ceram. Soc.* 70 (4) (1987) 237–241.
- [17] G.D. Mahan, Intrinsic defects in ZnO varistors, *J. Appl. Phys.* 54 (7) (1983) 3825–3832.
- [18] J.F. Cordaro, Y. Shin, J.E. May, Bulk electron traps in zinc oxide varistors, *J. Appl. Phys.* 60 (12) (1986) 4186–4190.
- [19] L.M. Levinson, H.R. Philipp, The physics of metal oxide varistors, *J. Appl. Phys.* (46) (1975) 1332–1341.